Vacuum-UV negative photoion spectroscopy of CF3Cl, CF3Br, and CF3I

Simpson, Matthew; Tuckett, Richard; Dunn, KF; Hunniford, CA; Latimer, CJ

DOI:
10.1063/1.3137103

Vacuum-UV negative photoion spectroscopy of CF_3Cl, CF_3Br and CF_3I

M.J. Simpson, R.P. Tuckett, K. Dunn, C. A. Hunniford and C. J. Latimer

J. Chem. Phys., (2009) **130**, 194302-1 – 194302-11

DOI : 10.1063/1.3137103

Professor Richard Tuckett (University of Birmingham) / July 2011

Vacuum-UV negative photoion spectroscopy of CF_3Cl, CF_3Br and CF_3I

(resubmitted after referees' comments : 23.4.09) A09.02.0114R

M. J. Simpson and R. P. Tuckett,*

School of Chemistry, University of Birmingham, Edgbaston, Birmingham B15 2TT, United Kingdom

K. F. Dunn, C. A. Hunniford and C. J. Latimer

Department of Physics and Astronomy, Queen's University Belfast, Belfast BT7 1NN, United Kingdom

Number of pages : 26 (excluding tables, figures and figure captions)
Number of tables : 2
Number of figures : 6

* Author for correspondence, tel +44 121 414 4425, fax +44 121 414 4403, email r.p.tuckett@bham.ac.uk

---

Abstract Using synchrotron radiation negative ions have been detected by mass spectrometry following vacuum-UV photoexcitation of trifluorochloromethane (CF_3Cl), trifluorobromomethane (CF_3Br) and trifluoroiodomethane (CF_3I). The anions F^-, X^-, F_2^-, FX^-, CF^-, CF_2^- and CF_3^- were observed from all three molecules, where X = Cl, Br or I, and their ion yields recorded in the range 8-35 eV. With the exception of Br^- and I^-, the anions observed show a linear dependence of signal with pressure, showing that they arise from unimolecular ion-pair dissociation. Dissociative electron attachment, following photoionization of CF_3Br and CF_3I as the source of low-energy electrons, is shown to dominate the observed Br^- and I^- signals, respectively. Cross sections for ion-pair formation are put on to an absolute scale by calibrating the signal strengths with those of F^- from both SF_6 and CF_4. These anion cross sections are normalized to vacuum-UV absorption cross sections, where available, and the resulting quantum yields are reported. Anion appearance energies are used to calculate upper limits to 298 K bond dissociation energies for $D^o(CF_3–X)$ which are consistent with literature values. We report new data for $D^o(CF_2I^+–F) \leq 2.7 \pm 0.2$ eV and $\Delta_f H^o_{298}\,(CF_2I^+) \leq (598 \pm 22)$ kJ mol^{-1}. No ion-pair formation is observed below the ionization energy of the parent molecule for CF_3Cl and CF_3Br, and only weak signals (in both I^- and F^-) are detected for CF_3I. These observations suggest neutral photodissociation is the dominant exit channel to Rydberg state photoexcitation at these lower energies.

I. INTRODUCTION

Ion-pair formation from a molecule is a unimolecular dissociation reaction in which two of the fragments produced are ionic; a cation-anion pair is formed. It is one of many ways in which a molecule releases energy following photoexcitation. Photoexcited states, usually Rydberg in character, may predissociate into ion pairs. This *indirect* mechanism is more favourable than *direct* ion pair photodissociation, based on Frank-Condon arguments and experimental results.[1] The formation and detection of ion pairs, therefore, can provide information on the electronic structure of a molecule and the decay dynamics of excited states. Our interest in the CF_3X series of substituted methanes, where X = Cl, Br, or I, is primarily fundamental – to compare the data and see the effects and resulting trends of changing substituent X. The interest in these molecules, however, is also environmental as CF_3Cl, CF_3Br, and CF_3I are all greenhouse gases and potential ozone depleters. The use of these molecules in industrial applications has inevitably led to their release into the atmosphere. For example, CF_3Cl (CFC-13) was used as a refrigerant and CF_3Br (halon 1301) as a fire suppressor, but both are now banned in accordance with the Montreal Protocol.[2] CF_3I is considered less environmentally unfriendly than CF_3Cl or CF_3Br and it is expected to have a relatively low atmospheric lifetime due to the weak C-I bond.[3] This property increases the potential for CF_3I applications, for example, as a plasma etching gas[4] and as a possible replacement for CF_3Br in fire extinguishing systems.[5]

This series of CF_3X molecules have C_{3V} symmetry, and the main effect of a change in the substituent X is the elongation and subsequent weakening of the C-X bond. The effect on the overall electronic structure of the molecule on changing X is not dramatic, since the orbitals of the X atom show little mixing with the CF_3 orbitals. The evidence for this property is best observed from photoelectron spectroscopy, where HeI, HeII and threshold photoelectron (TPE) spectra have been reported for CF_3Cl, CF_3Br and CF_3I.[6-11] Bands observed in the spectra from ionization of an X lone pair or a C-X bonding electron shift to lower energy as X gets larger. However, bands observed from ionization of an F lone pair or a C-F bonding electron are very similar in energy for CF_3Cl, CF_3Br and CF_3I. Absorption data on CF_3Cl have been well studied by photoabsorption spectroscopy[12,13] and electron energy loss spectroscopy (EELS).[14,15] More recent

absorption[16] and EELS[17] studies compare data for all three CF_3X molecules. While most of this work is restricted to energies < 15 eV, absorption data for CF_3Cl is reported up to 25 eV,[13,18] and for CF_3Br up to 30 eV.[18] Vacuum-UV fluorescence spectroscopy has also been studied for CF_3X molecules, where X = F, H, Cl, and Br (Ref. 19) and where X = F, H, Cl, Br, and I (Ref. 18).

In this paper we report data on the negative ions formed following vacuum-UV (VUV) photoexcitation of CF_3Cl, CF_3Br and CF_3I, and ion yields have been recorded as a function of photon energy in the range 8-35 eV using synchrotron radiation. Absolute cross sections for anions attributed to ion-pair formation have been evaluated using the negative ion data of CF_4 and SF_6 reported by Mitsuke *et al*.,[20,21] and quantum yields have been calculated from photoabsorption data.[16,18] The VUV photoion-pair formation of CF_3Cl has been studied previously using a quadrupole mass analyser by Schenk *et al*.,[22] but to our knowledge this is the first report of ion-pair production following photoexcitation of CF_3Br and CF_3I.

II. EXPERIMENTAL

The tunable VUV radiation was provided by a 1 m Wadsworth monochromator on Beamline 3.1 at the UK Daresbury Synchrotron Radiation Source (SRS). This beamline is optimized for high flux in the 8–35 eV region of the electromagnetic spectrum.[23] All the spectra were recorded with a modest resolution of 0.6 nm. The experimental apparatus used for the detection of negative ions has been described in detail elsewhere,[24] and only a brief description is provided here. The gas under study is injected *via* a needle generating a directed jet which bisects orthogonally the incident photon beam. The crossing point, which dictates the centre of the interaction region, is positioned in the middle of two grids on the third orthogonal axis. A potential difference across the grids sweeps negative ions along this axis towards a 3-element electrostatic lens for focusing, and into a Hiden Analytical HAL IV triple quadrupole mass spectrometer (QMS) for mass selection. Detection is achieved by a channeltron electron multiplier. Sensitivity is considerably enhanced by differential pumping which reduces the number of free electrons and secondary collisions in the QMS.

The relative photon flux is measured using a sodium salicylate window and visible photomultiplier tube combination. The apparatus and QMS, connected *via* a 1 mm diameter aperture, are pumped separately by turbo pumps which are backed by a common rotary pump, and the base pressure of the apparatus is ~10^{-7} mbar. With sample gas running, the typical pressure in the chamber is ~10^{-5} mbar. The pressure inside the chamber was measured using an ionization gauge, the sensitivity of which to CF_3Cl, CF_3Br, and CF_3I is calibrated in a separate experiment relative to N_2 gas using a capacitance manometer. Detected anion signals are initially recorded as a function of sample gas pressure over the range (0.5–5.0) × 10^{-5} mbar. Anions which show a *linear* dependence of signal with pressure most likely arise from unimolecular dissociation, and are attributed to ion-pair formation. Anions which show a *non-linear* dependence with pressure cannot be assigned as ion-pair products, and their signal is most likely influenced by secondary processes. For all anions produced from CF_3Cl, CF_3Br, and CF_3I, ion yields were recorded from 8–35 eV. For all scans presented below 11.8 eV (or 105 nm) a LiF window has been inserted to eliminate higher-order radiation. Gas samples were obtained from Apollo Scientific with a quoted purity of > 99% and were used without further purification.

The ion yields are presented as anion cross sections, σ, in units of cm^2. The method for obtaining these absolute measurements is identical to that from another recent ion-pair study, and is described in detail elsewhere.[25] In summary, the anion signal strengths (in counts s^{-1}) are normalized to relative photon flux, gas pressure, ring current and relative mass sensitivity of the quadrupole. The F^- signals from both CF_4 and SF_6 are also recorded and normalized as described above. The corrected signal for F^- from SF_6 is then normalized to the known cross section at 14.3 eV, (7 ± 2) × 10^{-21} cm^2 (Ref. 21). Likewise, the corrected signal for F^- from CF_4 is normalized to its value at 13.9 eV, (1.25 ± 0.25) × 10^{-21} cm^2 (Ref. 20). A multiplication factor, *k*, is obtained which coverts the arbitrary normalized signals into the quoted absolute values. In theory, the values *k* (F^-/SF_6) and *k* (F^-/CF_4) should then be equal, but in fact they differ by a factor of 1.6. Given the number of corrections made to the anion signals, this difference seems a reasonable

representation of experimental error. An average of the two k values is then used to determine absolute cross sections for the CF_3X anion signals. We comment that, whilst these values of anion cross sections probably have an error as high as ± 50–100 %, such *absolute* measurements are notoriously difficult to make and prone to errors which are often underestimated in the literature. These corrections are not made to anion signals which show a *non*-linear dependence on pressure (i.e. which are *not* formed by ion-pair formation), because one of the requirements is to correct for gas pressure.

III. THERMOCHEMISTRY: GENERAL COMMENTS

Our work also determines appearance energies (AE) at 298 K for many fragment anions from CF_3Cl, CF_3Br, and CF_3I and we compare these values with those calculated from thermochemical data. Berkowitz noted that, for many polyatomic molecules, a calculated threshold energy provides a lower limit to the experimental AE of an anion when suitable assumptions are made about the nature of the accompanying cation and / or neutral fragments.[1] However, usually there is equality in these two values, although *energy* and *enthalpy* are often indistinguishable words. In comparing our experimental AE values of anions with calculated enthalpies of appropriate dissociation reactions, we make two assumptions which are justified at the relatively modest resolution of our experiment, *ca.* 0.1–0.2 eV. First, although it is not accurate to equate an AE_{298} to the enthalpy of the corresponding unimolecular reaction at 298 K because of thermal effects,[26] the corrections needed to the AE_{298} values are typically only 0.05–0.15 eV, and we feel justified in ignoring them. Second, the effects of entropy are disregarded in our calculations, even though all unimolecular reactions involve $\Delta n > 0$, where Δn is the number of product species minus the number of reactant species. Thus $\Delta_r S^o_{298}$ will be positive, and $\Delta_r G^o_{298}$ for the unimolecular reactions will be more negative than the calculated $\Delta_r H^o_{298}$ values.

We use heats of formation, $\Delta_f H^o_{298}$, to calculate dissociation enthalpies. The majority of these values are obtained from the JANAF tables.[27] Data obtained from other sources are listed below, in kJ mol^{-1}. The

parent molecule $\Delta_f H^o_{298}$ values, for CF_3Cl, CF_3Br, and CF_3I are taken as −709, −650, and −586, respectively, from the work of Ruscic *et al*.[28] In calculations for F^-, we use the value of −249 using the electron affinity (EA) reported by Blondel *et al*.,[29] and for F_2^-, the value of −301 which uses the EA reported by Artau *et al*.[30] The values used for Cl^-, Br^- and I^- are −227, −213, and −188, respectively, which use experimental EAs from a recent review paper.[31] For CF^- we use a value of −63, using the EA(CF) = 3.3 ± 1.1 eV (reported as a lower limit),[32] and for CF_2^- a value of −199 which uses the EA(CF_2) = 0.179 ± 0.005 eV.[31] For CF_3^-, we calculate $\Delta_f H^o_{298}$ = −642 kJ mol^{-1} (Refs. 28 and 33). For CF_3^+ we take the value of +406 reported by Garcia *et al*.[34] For CCl^+ and $CFCl^+$ we use +1311 and +1101, respectively.[22] For CF_2Cl^+ we use the value from Creasy *et al*.,[10] +526, but note this uses a 0 K heat of formation of CF_2Cl. For $\Delta_f H^o_{298}$ (CF_2Br^+), we use the upper-limit value of 570 kJ mol^{-1} quoted by Seccombe *et al*.[35]

IV. RESULTS AND DISCUSSION

The negative ion mass spectra for the three CF_3X (X = Cl, Br, I) molecules recorded with white light at 0 nm all show the presence of the same seven anions; F^-, X^-, F_2^-, FX^-, CF^-, CF_2^- and CF_3^-. F^- and X^- are always the strongest signals. The remaining five anions were detected just above the sensitivity of the apparatus, the signals being ≤ *ca.* 2% of that of the dominant anion (F^- or X^-). It was observed that the X^- relative signal strengths increased with increasing mass and size of X; Cl^- = 18%, Br^- = 37% and I^- = 100% from CF_3Cl, CF_3Br and CF_3I, respectively, of the strongest anion signal (F^- from CF_3Cl and CF_3Br, I^- from CF_3I). Of all the anions, only FI^- was too weak to record as a function of photon energy. Negative ion yields for all other anions are presented below.

To our knowledge this is the first report of ion pair formation from CF_3Br and CF_3I. Similar experiments on CF_3Cl, however, have been reported in the literature.[22,36] Of particular relevance to our study is the work of Schenk *et al*.,[22] who also investigated the valence region of CF_3Cl with VUV synchrotron radiation, and

comparisons between the two sets of results are detailed in the discussion below. In summary, Schenk *et al.* were only able to detect F^-, Cl^- and CF_3^-. CF_3^- was detected with low intensity and an ion yield was not recorded. The F^- and Cl^- ion yields are in excellent agreement with the results presented here.

A. F^- from CF_3Cl, CF_3Br and CF_3I

The F^- ion yields from CF_3Cl, CF_3Br and CF_3I are presented in Figure 1 in the photon energy range 8-32 eV. For comparative purposes Figure 1 also includes the total photoabsorption spectrum,[18] threshold photoelectron spectrum[10] (TPES) and total fluorescence yield[18] for CF_3Cl and CF_3Br, and the TPES[11] and total fluorescence yield[18] for CF_3I. The corresponding numerical data from the F^- ion yields is presented in Table I. The small rise in signal at 12 eV seen in the F^- ion yields from CF_3Cl and CF_3Br is considered to result from second-order radiation, and is exaggerated by normalization to photon flux which is low at this energy. In all three cases the F^- signal showed a linear rise with gas pressure, indicating that F^- ions are formed by unimolecular ion-pair dissociation.

1. Onsets and thermochemistry

The F^- ion yield from CF_3Cl shows a gradual onset. The first indication of a rise in signal above the background is at 16.0 ± 0.2 eV (Figure 1, Table I). In the earlier work of Schenk *et al*. the F^- ion yield from CF_3Cl was reported with a wavelength resolution of 2 Å.[22] They report the onset of F^- ions to be 15.9 ± 0.3 eV, correlating this onset to reaction (1) using thermochemical calculations:

$$CF_3Cl \rightarrow F^- + CF_2^+ + Cl \qquad (1)$$

Schenk *et al*. also report second (16.8 ± 0.1 eV), third (18.2 ± 0.1 eV) and fourth (20.0 ± 0.1 eV) onsets corresponding to the dissociation reactions (2), (3) and (4), respectively.

$$CF_3Cl \rightarrow F^- + CFCl^+ + F \quad (2)$$

$$CF_3Cl \rightarrow F^- + CF^+ + F + Cl \quad (3)$$

$$CF_3Cl \rightarrow F^- + CCl^+ + 2F \quad (4)$$

Our thermochemical analysis, as outlined in Section III, agrees with all these assignments. However, the lack of well-defined onsets and features in the F^- ion yield from CF_3Cl, combined with the number of different dissociation channels possible, does not allow these assignments to be made with confidence. For example, the calculated dissociation enthalpies for producing the ion pairs $F^-/CFCl^+$ (+ F) [reaction (2)] and F^-/Cl^+ (+ CF_2) are 17.0 and 17.1 eV, respectively. Not only are both these values *higher*, and not lower, in energy than the second onset, but from this analysis alone both are equally valid assignments.

The F^- ion yield from CF_3Br shows the first onset at 14.7 ± 0.2 eV (Figure 1, Table I) which correlates best to the dissociation enthalpy of 14.9 eV calculated for reaction (5):

$$CF_3Br \rightarrow F^- + CF_2^+ + Br \quad (5)$$

For the same reasons as discussed above in the thermochemical analysis of F^- from CF_3Cl, even tentative assignments of other unimolecular dissociation reactions to onsets of features in the F^- ion yield from CF_3Br are not suggested here.

Assignments of dissociation processes to onsets in the F^- ion yield from CF_3I can be made more confidently; calculated thresholds for reactions (6), (7), (8) and (9) coincide with local minima, and hence with onsets to features in the ion yield [Figure 1(c)].

$$CF_3I \rightarrow F^- + CF_2^+ + I \quad (6)$$

$$CF_3I \rightarrow F^- + CF^+ + FI \quad (7)$$

$$CF_3I \rightarrow F^- + FI^+ + CF \quad (8)$$

$$CF_3I \rightarrow F^- + I^+ + CF + F \quad (9)$$

The calculated enthalpies for reactions (6-9) are 14.2, 14.3, 15.7 and 18.5 eV, respectively. It is likely that features in the ion yield which occur just after these values represent the 'turning on' of the newly-available dissociation channel(s). In addition, the sharp onset observed at 12.7 ± 0.2 eV [Figure 1(c)] can be correlated to formation of the F^-/I^+ (+ CF_2) ion pair - although this assignment is made more tentatively since the calculated enthalpy is 13.2 eV, 0.5 eV *above* this onset.

The lowest energy ion-pair reaction which yields F^- must be:

$$CF_3X \rightarrow F^- + CF_2X^+ \ (X = Cl, Br, I) \quad (10)$$

Lack of reliable information for $\Delta_f H^o(CF_2I^+)$ prevented a dissociation enthalpy for CF_3I in reaction (10) to be calculated. For CF_3Cl and CF_3Br the calculated thresholds for this reaction are 10.2 and ≤ 10.1 eV, respectively. In both cases these calculated dissociation enthalpies are significantly below the experimentally-observed appearance energy (AE) of F^- ions; the AE's are 16.0 and 14.7 eV for F^- from CF_3Cl and CF_3Br, respectively (Figure 1, Table I). There is therefore no evidence, from this thermochemical analysis, that F^- ions produced from CF_3Cl and CF_3Br arise *via* reaction (10). The AE for F^- from CF_3I, however, is much lower, at 9.7 eV (Figure 1, Table I). Even though a threshold energy could not be calculated for reaction (10) when X = I, it is the only ion-pair channel forming F^- from CF_3I that is likely to occur at energies below *ca.* 13 eV. The peak at 9.8 eV in the F^- ion yield from CF_3I, albeit very weak, must therefore arise from reaction (10).

2. *Discussion of the F^- spectra*

The photoabsorption spectra of CF_3Cl [Figure 1(a)] and CF_3Br [Figure 1(b)][18] extend over the energy range where F^- ions are observed from the two molecules. Figure 1 does not include a photoabsorption spectrum for CF_3I and published data in the energy range of interest (up to 25 eV) is limited.

The peak centred at 16.32 eV in the CF_3Cl absorption spectrum has been assigned as a transition to a 3s Rydberg orbital coverging on the fifth excited valence state of CF_3Cl^+ ($\tilde{E}\,^2A_1$).[18] From electron energy-loss spectroscopy (EELS) of CF_3Cl, King and McConkey have assigned observed features at 16.29, 17.1 and 18.2 eV as transitions to 3s, 3p and 3d Rydberg orbitals, respectively, all converging to CF_3Cl^+ ($\tilde{E}\,^2A_1$).[14] These features occur in the same energy range where the gradual onset of F^- ions from CF_3Cl is observed. The cross section for F^- ions in this energy range is relatively small (6×10^{-22} cm^2 at 17.6 eV) and well-defined peaks are not observed. As a result, and given the tentative nature of the assignments made from the photoabsorption and EEL spectra, we consider assigning the same transitions to the F^- ion yield as speculative. The one peak we do observe at 21.0 eV has not been clearly observed in the absorption spectrum.[18] It may correspond to a Rydberg state of CF_3Cl converging on either the $\tilde{F}\,^2E$ or $\tilde{G}\,^2A_1$ state of the parent ion. The above discussion assumes the formation mechanism is predissociative, yet direct excitation to the ion-pair state should not be discounted. The gradual onset and small cross section indicate weak Frank-Condon overlap, and therefore direct ion-pair formation is plausible. If this is the case, the AE of F^- ions may exceed the thermochemical ion-pair dissociation threshold by a greater amount than that from a predissociation mechanism where these two energies are more likely to be similar (Section III).

The feature in the CF_3Br photoabsorption spectrum at 15.96 eV has been assigned as a transition to a 4d Rydberg orbital converging on the fourth excited valence state of CF_3Br^+ ($\tilde{D}\,^2E$).[18] It is close in energy to the first observable peak in the F^- ion yield at 16.1 eV, and it is possible these two features share the same primary excitation process. The peak at 9.8 eV in the F^- ion yield from CF_3I is very sharp and weak, and

appears anomalous by comparison to the rest of the spectrum. The abrupt nature of this feature points to a predissociative mechanism and the low cross section could indicate the extent of overlap between states is small. It has been suggested, albeit tentatively, that Rydberg states of the n*s* series converging to the $\tilde{X}\,^2E_{3/2}$ ionization limit lie in this energy region. Indeed there is a strong absorption band between 9.4 and 9.9 eV showing detailed structure.[16]

It is generally accepted that the $\tilde{X}\,^2E$ electronic states of the CF_3X^+ (X = Cl, Br, I) cations result from ionization of X lone pair electrons, and the $\tilde{A}\,^2A_1$ from ionization of a C-X bonding electron.[6-9] The $\tilde{B}$, $\tilde{C}$, $\tilde{D}$, $\tilde{E}$ and $\tilde{F}$ electronic states of the cations between 15 and 22 eV are most likely from fluorine lone-pair excitations. It is expected that the bonding character of the fluorine lone-pair electrons will increase with increasing ionization energy.[8] Photoexcitation of these electrons leads to the production of F^- anions. Only F^- produced from CF_3I is observed following photoexcitation of an electron associated with the X substituent. Even so, the resulting single peak at 9.8 eV appears isolated and the cross section is very small compared to the rest of the spectrum. The similarities of the photoelectron spectra for the three CF_3X molecules have been highlighted by Cvitaš *et al.*,[6,8] and they suggest that changing substituent X affects the electronic structure of the CF_3 group very little. Despite this observation, the F^- ion yields from these three molecules differ significantly. The extent of structure and the energy range over which F^- is observed increases as X changes from Cl through to I. In addition, the AE of F^- ions decreases. These trends appear more significant when substituting Br for I than when substituting Cl for Br. This trend possibly reflects the differing polarizabilities of the halogen atoms; the values are 2.18, 3.05 and 5.35×10^{-24} cm^3 for neutral atomic Cl, Br and I, respectively.[37]

B. X^- from CF_3X (X = Cl, Br, I)

1. Cl^- from CF_3Cl

The Cl^- ion yield from CF_3Cl is shown in Figure 2 from 12-34 eV. For comparative purposes Figure 2 also includes the total photoabsorption spectrum,[18] threshold photoelectron spectrum[10] (TPES) and total fluorescence yield[18] for CF_3Cl. The numerical information is summarized in Table I. The signal in the Cl^- ion yield observed between 12 and 14 eV is considered to result from second-order effects, which are exaggerated when flux normalizing the spectrum. The Cl^- signal was shown to change linearly with CF_3Cl gas pressure, indicating that the mechanism for Cl^- formation is unimolecular ion-pair dissociation.

The lowest energy ion-pair fragmentation leading to Cl^- production must also produce the cation CF_3^+:

$$CF_3Cl \rightarrow Cl^- + CF_3^+ \quad (11)$$

The calculated enthalpy for (11) is 9.2 eV. However, the experimentally-observed onset to Cl^- production from CF_3Cl is 16.1 ± 0.2 eV. In the earlier work of Schenk *et al.*[22] a value of 16.0 ± 0.1 eV is reported, in excellent agreement with the present work. The observed Cl^- signal at onset may be assigned to the following dissociation reaction:

$$CF_3Cl \rightarrow Cl^- + CF_2^+ + F \quad (12)$$

The calculated enthalpy change for reaction (12) is 15.4 eV. Other onsets to features in the Cl^- ion yield, observed at 18.4, 21.3, and 23.4 eV (Figure 2), occur where a different fragmentation reaction becomes energetically accessible:

$$CF_3Cl \rightarrow Cl^- + CF^+ + 2F \quad (13)$$

$$CF_3Cl \rightarrow Cl^- + F^+ + CF_2 \quad (14)$$

$$CF_3Cl \rightarrow Cl^- + F_2^+ + CF \quad (15)$$

The calculated enthalpy changes for reactions (13-15) are 18.4, 21.4, and 23.3 eV, respectively. We note that an experimental onset occurring at a calculated thermochemical threshold suggests there is good overlap between an excited intermediate state and the new exit channel which has energetically become open.

The production of Cl^- has similarities to that of F^- from CF_3Cl; the fragmentation reaction assumed to occur at onset [reaction (12)] is almost identical to that assigned to F^- anions from CF_3Cl [reaction (1)]. Both ion yields show a very similar AE (Table 1) and in both cases this value is much higher than the lowest-energy dissociation reaction to form the respective anion as an ion pair [reactions (10) and (11)]. In addition, the cross sections for F^- and Cl^- production peak at almost identical energies (Table I), and in the range 16-18 eV the cross sections are comparable. For example, at 17.5 eV, $\sigma_{F^-} = 5.4 \times 10^{-22}$ cm^2 and $\sigma_{Cl^-} = 9.2 \times 10^{-22}$ cm^2. Above 18 eV F^- formation increases with respect to Cl^- anions; at 21.0 eV, $\sigma_{F^-} = 1.5 \times 10^{-20}$ cm^2 and $\sigma_{Cl^-} = 2.2 \times 10^{-21}$ cm^2.

2. Br^- from CF_3Br and I^- from CF_3I

The Br^- and I^- ion yields from CF_3Br and CF_3I, respectively, are shown in Figure 3 in the range 8-28 eV. The threshold photoelectron spectra for CF_3Br (Ref. 10) and CF_3I (Ref. 11) are superimposed in red above the ion yields for comparative purposes. When recorded as a function of gas pressure, both the Br^- and I^- signals change *non*-linearly; the rate of change in anion signal increases pseudo-exponentially with increasing pressure. When this trend has been seen before (*e.g.* SF_5^- from SF_6 and SF_5CF_3) the anions have been shown to arise from dissociative electron attachment, following photoionization of the parent molecule as the source of low-energy electrons.[25] The same conclusion is reached in this study for the formation of Br^- and I^- ions from CF_3X (X = Br, I). The two-step mechanism is shown below:

$$CF_3X + h\nu \rightarrow CF_3X^+ + e^- \quad (16)$$

$$CF_3X + e^- \rightarrow X^- + CF_3 \quad (17)$$

CF_3Br (Refs. 38 and 39) and CF_3I (Refs. 4 and 40) are both known to attach electrons rapidly; the recommended values for the thermal electron attachment rate coefficients are 1.4×10^{-8} cm^3 s^{-1} for CF_3Br (Ref. 38) and 1.9×10^{-7} cm^3 s^{-1} for CF_3I (Ref. 4). In addition, the Br^- and I^- ion yields show similarities to the threshold photoelectron spectra for CF_3Br and CF_3I, respectively (Figure 3). These similarities are much more obvious between the I^- ion yield and CF_3I TPES, which perhaps reflects the difference in magnitude between the attachment rate coefficients for CF_3Br and CF_3I. The apparent lack of agreement between the two spectra (ion yield *vs* TPES) at lower photon energies in both molecules is interesting. Only background signal is observed in the Br^- ion yield over the photon energy range, 12-15 eV, where the first two bands can be seen in the CF_3Br TPES. The first bands in the CF_3I TPES, representing the spin-orbit split ground state of CF_3I^+, $\tilde{X}\,^2E_{3/2}$ and $\tilde{X}\,^2E_{1/2}$ are only observed very weakly in the I^- spectrum; in Figure 3(b) the I^- signal over this energy region has been enlarged by a factor of 30. The ion yields of Figure 3 are unlikely to result from dissociative electron attachment alone; Br^- or I^- anions produced by ion-pair dissociation are also detected. How much of either anion signal is due to dissociative electron attachment, and how much to ion-pair formation is unknown. However, given the evidence above it is clear that dissociative electron attachment is the more dominant mechanism contributing to the Br^- and I^- ion yields.

The agreement between the TPES and the Br^-/I^- yield is slightly better at the higher energies scanned in Figure 3, and the absence of the low-energy bands between 12-15 eV in the Br^- channel from CF_3Br, and the relative weakness of the analogous bands in the I^- channel from CF_3I, remain unexplained. Likewise, the reasons why the relative intensities between ion yield and TPES spectra are different, including the relative intensities of the $\tilde{X}\,^2E_{3/2}$ and $\tilde{X}\,^2E_{1/2}$ spin-orbit sub-bands in CF_3I^+, is unclear. We note that the SF_6^- yield

from SF_6 and the SF_5^- yield from SF_5CF_3 are both dominated by the two-step electron attachment mechanism over the *whole* of the valence region, and the anion yield and TPES show better agreement over a wider range of energies.[25] There is limited evidence from work on other polyatomic molecules (*e.g.* c-C_5F_8) that the agreement between the two spectra is enhanced if electron attachment is *non*-dissociative.[25]

For electron attachment to occur, the parent molecule must first be ionized. Therefore, at energies below the onset to ionization any anions produced can only arise from ion-pair dissociation. This is observed in the ion yield for I^- from CF_3I. The onset to ionization in CF_3I is 10.3 eV.[41,42] However, the experimentally-determined onset to I^- formation is at 8.8 ± 0.2 eV and a discrete peak in the signal results at 9.0 eV [Figure 3(b)]. Thermochemical calculations suggest the only possible ion-pair dissociation reaction which produces I^- at this energy is (18):

$$CF_3I \rightarrow I^- + CF_3^+ \qquad (18)$$

The calculated enthalpy change for reaction (18) is 8.3 eV. We determine the cross section for I^- ion-pair formation at 9.0 eV to be 3.8×10^{-21} cm^2. Normalizing this value to the total photoabsorption cross section at 9.0 eV[16] gives a quantum yield of *ca.* 8×10^{-5}. An analysis of the photoabsorption spectrum of CF_3I has suggested that Rydberg states of the n*s* series converging to the $\tilde{X}\,^2E_{3/2}$ ionization limit lie in this energy region, and absorption features showing vibrational structure have been observed centred at energies 8.8 and 9.5 eV.[16]

C. F_2^- and FX^- (X = Cl, Br) from CF_3Cl, CF_3Br and CF_3I

The F_2^- ion yields from CF_3X (X = Cl, Br, I) and the FX^- (X = Cl, Br) yields from CF_3Cl and CF_3Br in the range 12-34 eV are shown in Figures 4 and 5, respectively. All these anion signals show a linear increase when recorded as a function of gas pressure, indicating that F_2^- and FX^- result from unimolecular

photodissociation. The Figures report absolute cross sections for these processes and further numerical information is provided in Table I. The cross sections for production of FCl^-, FBr^- and F_2^- from CF_3X are up to three orders of magnitude smaller compared to F^- production (Table I).

The onsets for F_2^- production, *ca.* 21, 19 and 17 eV for X = Cl, Br, I, occur at the thermochemical thresholds for the ion pair dissociation reaction shown below:

$$CF_3X \rightarrow F_2^- + X^+ + CF \ (X = Cl, Br, I) \qquad (19)$$

The calculated dissociation enthalpy changes for (19) are 21.1, 19.2, and 17.2 eV for X = Cl, Br, and I, respectively. Two cautionary points should be made. First, the uncertainty in the values of the experimentally-determined onsets (Table I, Figure 4) is degraded by the poor signal/noise ratio in the ion yields. Second, an energy barrier resulting from forming a new F-F bond is likely. If so, the true thermochemical threshold will lie below the experimental onset, and other lower-energy dissociation reactions should be considered (*e.g.* F_2^-/CF^+ ion pair formation). A similar discussion on the dissociation reactions leading to FCl^- and FBr^- from CF_3Cl and CF_3Br, respectively, is not possible due to the lack of data on the electron affinities of FCl and FBr.

The F_2^- ion yields all show one major feature which most likely represents the presence of a Rydberg state converging to the fifth ($\tilde{E}$) or sixth ($\tilde{F}$) excited valence states of the CF_3X^+ molecules. As discussed in Section IV.A. 2. the origin of the excited electron is from a fluorine lone pair with significant C-F bonding character. In all three F_2^- ion yields a tentative correlation can be made between the peak energy and features in the corresponding F^- ion yields. This is unsurprising considering two F atoms must be cleaved preceding the formation of F_2^-.

D. CF^-, CF_2^- and CF_3^- from CF_3Cl, CF_3Br and CF_3I

The CF^-, CF_2^- and CF_3^- ion yields from CF_3X (X = Cl, Br, I) are shown in Figure 6. Numerical information is given in Table I. All these anion signals all show a linear rise when recorded as a function of increasing gas pressure, indicating they result from unimolecular photodissociation. The cross sections for CF_n^- (n = 1-3) production are approximately two orders of magnitude smaller than those determined for F^- production (Table I).

Each CF_n^- (n = 1-3) anion from each parent CF_3X molecule shows only one feature in the ion yield, with the exception of CF^- from CF_3Cl which shows more features. We propose that the true onset for CF^- from CF_3Cl is 25.5 eV (Table I, Figure 6) and that the observed signal in the energy range 16-25 eV results from detecting Cl^- anions. We suggest two reasons for this. First, the mass-to-charge ratios (*m*/*z*) used when recording ion yields are close in value, 31 for CF^- and 35 for Cl^-. Although the Cl^- signal peaks at *m*/*z* 35, *weak* contributions can be detected at *m*/*z* values as low as 30. Combined with the fact that the CF^- signal relative to that of Cl^- is very weak, the Cl^- contribution at *m*/*z* 31 becomes significant. Second, the ion yield of Cl^- (Section B., Figure 2) and that of CF^- (Figure 6) from CF_3Cl appear similar in the 16-25 eV energy range; both ion yields show an onset around 16 eV, with featues at *ca*. 17.5 and 21 eV.

1. Onsets and thermochemistry

Unimolecular dissociation of CF_3X (X = Cl, Br, I) leading to CF_3^- formation must also produce the cation X^+:

$$CF_3X \rightarrow CF_3^- + X^+ \ (X = Cl, Br, I) \qquad (20)$$

The calculated thermochemical thresholds for reaction (20) are 14.9, 13.1, and 11.0 eV when X = Cl, Br, and I, respectively; the experimentally-determined onsets for CF_3^- anions are 15.5, 13.6, and 11.0 eV, respectively (Table I, Figure 6). A similar dissociation process most likely produces the CF_2^- anions:

$$CF_3X \rightarrow CF_2^- + X^+ + F \ (X = Cl, Br, I) \quad (21)$$

The calculated thermochemical thresholds for reaction (21) are 20.3, 18.5, and 16.4 eV when X = Cl, Br, and I, respectively; the experimentally-determined onsets for CF_2^- anions are 20.2, 18.2, and 16.0 eV, respectively (Table I, Figure 6). Dissociation of CF_3X (X = Cl, Br, I) to produce the CF_2^-/F^+ ion pair will only occur at excitation energies several eV *above* the experimental onset, and is therefore not possible. Dissociation to produce the CF_2^-/FX^+ ion pair, however, may occur *below* the experimental onset.

$$CF_3X \rightarrow CF_2^- + FX^+ \ (X = Cl, Br, I) \quad (22)$$

The calculated thermochemical thresholds for reaction (22) are 17.4, 15.9, and 13.6 eV when X = Cl, Br, and I, respectively. If reaction (22) occurs, 2-3 eV excess energy must be accounted for. An experimental onset is always considered an upper limit, and small amounts of energy will undoubtedly be converted into translational energy of the fragment species. It should also be considered that an energy barrier to FX^+ formation may exist, given that bonds are both broken and formed. Similar arguments are made in Section IV. C with respect to the anions F_2^- and FX^- (X = Cl, Br, I). We consider the more likely process producing CF_2^- from CF_3X is reaction (21), rather than reaction (22). Low excess energies favour the production of ion pairs,[1] and a bond-breaking-only dissociative reaction is favoured over one where bonds are additionally formed.

The considerations discussed above are also relevant in the discussion of the CF^- fragment anion. The possibilities for the associated fragment cation and neutral species are greater. Several diatomic fragments, F_2, F_2^+, FX or FX^+, could realistically be associated with CF^- ion-pair formation. The thermochemistry suggests all processes pairing CF^- formation with X^+, F^+ or F_2^+ could be contributing to the observed CF^- signal from CF_3X photodissociation as observed in Figure 6. This is perhaps reflected by the broad band which features in all three CF^- ion yields.

2. Discussion of the CF_n^- (n = 1-3) spectra

From observation of Figure 6 it is clear that interchanging the X substituent in CF_3X with Cl, Br, or I has little effect on the structure of the ion yields of CF^-, CF_2^-, or CF_3^-. However, there are consistent shifts in the appearance energy (AE) of CF_n^- to lower energy as X increases in size. For example, the shift in AE for each anion is almost exactly the same when substituting Cl for Br as when substituting Br for I (Table I); the AE(CF^-) from CF_3I is 2.0 eV lower in energy than AE(CF^-) from CF_3Br which is 1.9 eV lower than AE(CF^-) from CF_3Cl. This trend is expected because all anions are observed at their thermochemical threshold, whose values decrease as the size of X increases.

The broad nature of the features in the CF^- ion yields does not allow any direct comparisons to be made with other spectra. In addition, the energy required to yield CF^- from photoexciting CF_3X (X = Cl, Br, I) is comparatively large with respect to other negative ions. Intermediate excited Rydberg states at these energies probably converge on the first *inner*-valence excited state of CF_3X^+. Alternatively, these features may represent direct ion-pair formation with no involvement of an intermediate excited state. The energies of peak maxima in all the CF_2^- and CF_3^- ion yields, however, are similar to energies of features observed in other anion spectra, and likely represent common excited intermediate states and hence competing ion-pair dissociation channels.

V. BOND DISSOCIATION ENERGIES

The experimental appearance energies (AE) for anions determined by this work may be used to calculate upper limits to bond dissociation energies, D^o_{298}.[1] For example, using the AE of CF_3^- can provide an upper limit to $D^o(CF_3–X)$ if the ionization energy (IE) of X and the electron affinity (EA) of CF_3 are known, where X = Cl, Br, I:

$$AE(CF_3^-) \geq D^o(CF_3–X) + IE(X) – EA(CF_3) \quad (23)$$

Note that the $AE(CF_3^-)$ correlates to dissociation reaction (20). When the unimolecular dissociation involves multiple bond-breaking or the formation of a new bond, calculations performed in this way become over-complicated and too many assumptions are made. Therefore, only AE values for anions resulting from *single* bond-breaking ion-pair dissociation are considered here. The resulting upper limits to bond dissociation energies are presented in Table II and compared to literature values. In addition $D^o(CF_3–F)$ is calculated from the AE (F^- from CF_4)[25] and is also included in Table II. The uncertainty in the D^o upper limits calculated from these data is ± 0.2 eV which is taken directly from the estimated error in the AE values (Table I). The calculations for these values are explained in more detail below. We note the consistency between upper-limit values for $D^o(CF_3–X)$ obtained indirectly from this ion-pair work and the accepted literature values.[42] Furthermore, the upper-limit value for D^o tends towards the accurate value as the size of X increases from F through to I. This can possibly be explained by the density of Rydberg states of CF_3X increasing as the size of X increases, and therefore the increasing likelihood that the equality of equation (23) holds.

As shown in equation (23) the AE values for CF_3^- from CF_3X (Table I, Figure 6) are used to calculate $D^o(CF_3–X)$. The EA of the CF_3 radical is 1.82 ± 0.05 eV,[33] and the ionization energies for Cl (12.970 eV), Br (11.816 eV) and I (10.453 eV) are taken from the JANAF thermochemical tables.[27] The calculation is

slightly different for $D^o(CF_3–F)$ because CF_3^- was not observed from CF_4 (Ref. 25), but the AE(F^- from CF_4) can be used to yield the same information if we now use the EA(F) (3.401 eV)[29] and IE(CF_3) (9.04 ± 0.04 eV)[34] values instead.

The formation of F^- from CF_3I at onset arises from dissociation reaction (10). Unfortunately, because the IE(CF_2I) is currently not known, an upper limit to $D^o(CF_2I–F)$ cannot be calculated from the AE(F^-) value as described above. However, the relevant information is known in order to calculate an upper limit to $D^o(CF_2I^+–F)$ if equation (24) is considered:

$$AE(F^-) \geq IE(CF_3I) + D^o(CF_2I^+–F) – EA(F) \quad (24)$$

The AE(F^-) is 9.7 ± 0.2 eV (Table I, Figure 1), the IE(CF_3I) is 10.37 eV,[41] and the EA(F) is 3.401 eV,[29] giving $D^o(CF_2I^+–F) \leq 2.7 \pm 0.2$ eV or 263 ± 20 kJ mol^{-1}. If $D^o(CF_2I^+–F)$ is defined as the enthalpy change for reaction (25), which is valid if the Traeger and McLoughlin correction terms are ignored (Section III),[26] then an upper limit to $\Delta_f H^o_{298}$ (CF_2I^+) can be determined.

$$CF_3I^+ \rightarrow CF_2I^+ + F \qquad \Delta_r H^o_{298} \leq (263 \pm 20) \text{ kJ mol}^{-1} \quad (25)$$

Using thermochemistry already provided (Sections III and V) we calculate $\Delta_f H^o_{298}$ (CF_2I^+) ≤ (598 ± 22) kJ mol^{-1}.

VI. CONCLUSIONS

Negative ions have been detected following the photoexcitation of CF_3Cl, CF_3Br, and CF_3I in the photon energy range 8-35 eV. For the fast electron-attaching gases CF_3Br and CF_3I, the Br^- and I^- signals are heavily influenced by dissociative electron attachment. All other anions detected from these three molecules

result from ion-pair formation. A collection of the numerical data from this study is compiled in Tables I and II. We have shown that experimental AE values from ion-pair formation can be used to calculate upper limits for bond dissociation energies (Table II). This same point was made by Berkowitz in 1996,[1] but has rarely been implemented since. We report new data for $D^o(CF_2I^+–F) \leq 2.7 \pm 0.2$ eV and $\Delta_f H^o_{298}\,(CF_2I^+) \leq (598 \pm 22)$ kJ mol^{-1}.

The most surprising observation from this work is the lack of ion-pair formation detected at lower photon energies, particularly at energies below the ionization energy (IE) of the parent molecule. This anomaly is surprising because ion-pair fragmentation is energetically allowed and because significant structure is observed in the photoabsorption spectra below the IE. The best example of this is seen in $X^–$ ion pair formation from CF_3X (X = Cl, Br, I); a comparatively large cross section for $X^–$ produced by reaction (26) would be predicted, but the spectra show no contribution from $Cl^–$ or $Br^–$ anions produced in this way. $I^–$ anions, however, are observed below the IE of CF_3I but the signal is surprisingly weak.

$$CF_3X \rightarrow X^– + CF_3^+ \text{ (X = Cl, Br, I)} \qquad (26)$$

The total fluorescence yields and photoabsorption spectra correlate very little, and although there will be some contribution from fluorescence, it is not expected to be significant. Therefore, the structure observed in the photoabsorption spectra for CF_3Cl, CF_3Br, and CF_3I below the IE must almost exclusively result from neutral photodissociation. Finally, we note that ion-pair formation from CF_4 (Ref. 20, 25) shows completely different properties to the CF_3X molecules studied in this paper. This should not be surprising for two reasons. First, the symmetry of the molecule changes from T_d to C_{3v}. Second, the substitution of one F by a much heavier halogen atom increases the polarizability of the molecule, and therefore enhances its propensity to attach low-energy electrons.

ACKNOWLEDGEMENTS

We thank Dr. David Shaw for help in running experiments on beamline 3.1 at the Daresbury SRS, Dr Michael Parkes for help with data collection, and Prof. Ivan Powis for providing the threshold photoelectron data. We also thank Dr Sahangir Ali, whose Ph.D thesis provided photoabsorption and fluorescence spectra for this series of molecules. Finally, we thank Dr Michael Parkes for a critical reading of the manuscript. This collaboration between the groups in Birmingham and Belfast was partially funded by EPSRC Network Grant No. GR/N26234/01. CCLRC is thanked for the provision of SRS beamtime.

[1] J. Berkowitz, in *VUV and Soft X-Ray Photoionization*, edited by U. Becker and D. A. Shirley (Plenum, New York, 1996), p. 263.

[2] UNEP website, http://ozone.unep.org/.

[3] S. Solomon, J. B. Burkholder, A. R. Ravishankara and R. R. Garcia, J. Geophys. Res. D: Atmos. **99**, 20929 (1994).

[4] L. G. Christophorou and J. K. Olthoff, J. Phys. Chem. Ref. Data **29**, 553 (2000).

[5] Y. Li, K. O. Patten, D. Youn and D. J. Wuebbles, Atmos. Chem. Phys. **6**, 4559 (2006).

[6] T. Cvitaš, H. Güsten and L. Klasinc, J. Chem. Phys. **67**(6), 2687 (1977).

[7] R. Jadrny, L. Karlsson, L. Mattsson and K. Siegbahn, Physica Scripta **16**, 235 (1977).

[8] T. Cvitaš, H. Güsten, L. Klasinc, I. Novadj and H. Vančik, Z. Naturforsch **33a**, 1528 (1978).

[9] J. Doucet, P. Sauvageau and C. Sandorfy, J. Chem. Phys. **58**(9), 3708 (1972).

[10] J. C. Creasey, D. M. Smith, R. P. Tuckett, K. R. Yoxall, K. Codling and P. Hatherly, J. Phys. Chem. **100**(11), 4350 (1996).

[11] I. Powis, O. Dutult, M. Richard-Viard and P. Guyon, J. Chem. Phys. **92**(3), 1643 (1990).

[12] R. Gilbert, P. Sauvageau and C. Sandorfy, J. Chem. Phys. **60**(12), 4820 (1974).

[13] H. W. Jochims, W. Lohr and H. Baumgärtel, Ber. Bunsenges. Phys. Chem. **80**, 130 (1976).

[14] G. C. King and J. W. McConkey, J. Phys. B: At. Mol. Opt. Phys. **11**(10), 1861 (1978).

[15] J. W. Au, G. R. Burton and C. E. Brion, Chem. Phys. **221**, 151 (1997).

[16] S. Eden, P. Limão-Vieira, S. V. Hoffmann and N. J. Mason, Chem. Phys. **323**, 313 (2006).

[17] M. Hoshino, K. Sunohara, C. Makochekanwa, L. Pichl, H. Cho and H. Tanaka, J. Chem. Phys. **126**, 024303 (2007).

[18] S. Ali, Ph.D. thesis, University of Birmingham, 2007.

[19] H. Biehl, K. J. Boyle, R. P. Tuckett, H. Baumgärtel and H. W. Jochims, Chem. Phys. **214**, 367 (1997).

[20] K. Mitsuke, S. Suzuki, T. Imamura and I. Koyano, J. Chem. Phys. **95**, 2398 (1991).

[21] K. Mitsuke, S. Suzuki, T. Imamura and I. Koyano, J. Chem. Phys. **93**, 8717 (1990).

[22] H. Schenk, H. Oertel and H. Baumgärtel, Ber. Bunsenges. Phys. Chem. **83,** 683 (1979).

[23] C. R. Howle, S. Ali, R. P. Tuckett, D. A. Shaw and J. B. West, Nucl. Instrum. Methods Phys. Res. B **237**, 656 (2005).

[24] C. A. Hunniford, S. W. J. Scully, K. F. Dunn and C. J. Latimer, J. Phys. B **40**, 1225 (2007).

[25] M. J. Simpson, R. P. Tuckett, K. F. Dunn, C. A. Hunniford, C. J. Latimer and S. W. J. Scully, J. Chem. Phys. **128**, 124315 (2008).

[26] J. C. Traeger and R. G. McLoughlin, J. Am. Chem. Soc. **103**, 3647 (1981).

[27] M. W. Chase, J. Phys. Chem. Ref. Data Monogr. **9**, (1998).

[28] B. Ruscic, J. V. Michael, P. C. Redfern, L. A. Curtiss and K Raghavachari, J. Phys. Chem. A **102**, 10889 (1998).

[29] C. Blondel, C. Delsart and F. Goldfarb, J. Phys. B **34**, L281 (2001).

[30] A. Artau, K. E. Nizzi, B. T. Hill, L. S. Sunderlin and P. G. Wenthold, J. Am. Chem. Soc. **122**, 10667 (2000).

[31] J. C. Rienstra-Kiracofe, G. S. Tschumper, H. F. Schaefer, S. Nandi and B. Ellison, Chem. Rev. **102**, 231 (2002).

[32] J. C. J. Thynne and K. A. G. MacNeil, Int. J. Mass Spectrom. Ion Phys. **5**, 329 (1970).

[33] H. J. Deyerl, L. S. Alconcel and R. E. Continetti, J. Phys. Chem. A **105**, 552 (2001).

[34] G. A. Garcia, P. M. Guyon and I. Powis, J. Phys. Chem. A **105**, 8296 (2001).

[35] D. P. Seccombe, R. P. Tuckett and B. O. Fisher, J. Chem. Phys. **114**, 4074 (2001).

[36] S. W. J. Scully, Ph.D. thesis, Queen's University Belfast, 2004.

[37] D. R. Lide, *Handbook of Chemistry and Physics 88th Edition* (Taylor and Francis, London, 2007), Sec.10-p194-195.

[38] L. G. Christophorou, Z. Phys. Chem. **195**, 195 (1996).

[39] S. Marienfeld, T. Sunagawa, I. I. Fabrikant, M. Braun, M.-W. Ruf and H. Hotop, J. Chem. Phys. **124**, 154316 (2006).

[40] S. Marienfeld, I. I. Fabrikant, M. Braun, M.-W. Ruf and H. Hotop, J. Phys. B: At. Mol. Opt. Phys. **39**, 105 (2006).

[41] N. A. Macleod, S. Wang, J. Hennessy, T. Ridley, K. P. Lawley and R. J. Donovan, J. Chem. Soc., Faraday Trans. **94**, 2689 (1998).

[42] D. R. Lide, *Handbook of Chemistry and Physics 88th Edition* (Taylor and Francis, London, 2007), Sec.9-p63-64.

Table I. Appearance energies, cross sections and quantum yields for anions observed from photoexcitation of CF_3Cl, CF_3Br and CF_3I.

Molecule [AIE [a] (eV)]	Anion	AE [b] (eV)	Cross section maximum [c] (cm^2)	Energy [d] (eV)	Quantum yield [e]
CF_3Cl [12.4]	F^-	16.0	1.5×10^{-20}	21.0	1.8×10^{-4}
	Cl^-	16.1	2.3×10^{-21}	20.9	2.9×10^{-5}
	F_2^-	*ca.* 21 [f]	6.8×10^{-23}	22.7	8.5×10^{-7}
	FCl^-	*ca.* 18 [f]	6.5×10^{-23}	20.8	8.0×10^{-7}
	CF^-	25.5 [g]	1.6×10^{-22}	27.3	- [h]
	CF_2^-	20.2	1.5×10^{-22}	21.3	1.8×10^{-6}
	CF_3^-	15.5	2.8×10^{-22}	18.1	3.5×10^{-6}
CF_3Br [11.5]	F^-	14.7	9.7×10^{-21}	19.6	1.2×10^{-4}
	Br^-	15.1	- [i]	-	- [i]
	F_2^-	*ca.* 19 [f]	2.8×10^{-22}	20.4	3.4×10^{-6}
	FBr^-	*ca.* 18 [f]	5.5×10^{-22}	20.4	6.6×10^{-6}
	CF^-	23.6	3.4×10^{-22}	25.6	5.2×10^{-6}
	CF_2^-	18.2	4.9×10^{-22}	19.5	5.8×10^{-6}
	CF_3^-	13.6	2.5×10^{-22}	14.8	4.0×10^{-6}
CF_3I [10.4]	F^-	9.7	1.1×10^{-20}	20.4	- [j]
	I^-	8.8	- [i]	-	- [i]
	F_2^-	*ca.* 17 [f]	8.5×10^{-23}	20.1	- [j]
	CF^-	21.6	1.1×10^{-22}	23.6	- [j]
	CF_2^-	16.0	4.6×10^{-22}	16.8	- [j]
	CF_3^-	11.0	5.7×10^{-22}	12.7	- [j]

[a] Adiabatic ionization energy for CF_3Cl (Ref. 10), CF_3Br (Ref. 10) and CF_3I (Ref. 42).

[b] Observed appearance energy (AE) from this work. We estimate the error in the reported values to be ± 0.2 eV, based on the resolution and step size used to record the ion yields.

[c] Cross section for anion production following photoexcitation of the parent molecule.

[d] Energy of peak maximum at which cross section and quantum yield measurements are taken.

[e] Quantum yields for anion production, obtained by dividing cross sections for anions (column 4) by total photoabsorption cross sections. The latter values are given for CF_3Cl and CF_3Br (Ref. 18).

[f] Cannot state AE with any confidence due to poor signal/noise.

[g] There is some ambiguity surrounding the mass of anions detected contributing to the CF^- ion yield

from CF_3Cl. The signal observed in the range 16-25 eV is thought to arise from Cl^- ions (see text), and the value of 25.5 eV represents our interpretation of the true onset to CF^- ions.

[h] Quantum yield is not calculated because absolute photoabsorption data for CF_3Cl is not available at this energy.

[i] The Br^- and I^- ion yields are significantly influenced by anions arising from dissociative electron attachment and cross sections, and hence quantum yields, cannot be defined.

[j] Quantum yields cannot be calculated at this photon energy, because the available absolute photoabsorption data for CF_3I is limited to photon energies < 12 eV.

Table II. Upper limits to bond dissociation energies and comparisons with literature values.

Bond	D^o_{298} / eV	
	This work	Ref. 42
CF_3–F	≤ (7.4 ± 0.2) [a]	5.67
CF_3–Cl	≤ (4.4 ± 0.2) [b]	3.79
CF_3–Br	≤ (3.6 ± 0.2) [b]	3.07
CF_3–I	≤ (2.4 ± 0.2) [b]	2.36
CF_2I^+–F	≤ (2.7 ± 0.2) [c]	-

[a] Calculated from the appearance energy of F^- from CF_4 (Ref. 25).

[b] Calculated from the appearance energy of CF_3^- from CF_3Cl, CF_3Br, and CF_3I, respectively.

[c] Calculated from the appearance energy of F^- from CF_3I.

Figure Captions

Figure 1. Cross sections for F^- production following photoexcitation of (a) CF_3Cl, and (b) CF_3Br between 12 and 32 eV. The total photoabsorption spectra (Ref. 18), threshold photoelectron spectra (Ref. 10), and total fluorescence yields (Ref. 18) for CF_3Cl and CF_3Br are included for comparative purposes. (c) Cross section for F^- production following photoexcitation of CF_3I between 8 and 32 eV. The threshold photoelectron spectrum (Ref. 11, with permission of the authors) and total fluorescence yield (Ref. 18) are included for comparative purposes. All F^- ion yields were recorded with a step size of 0.1 eV and a wavelength resolution of 6 Å. This resolution is equivalent to 0.2 eV at 20.0 eV.

Figure 2. Cross section for Cl^- production following photoexcitation of CF_3Cl in the energy range 12-34 eV. The total photoabsorption spectrum (Ref. 18), threshold photoelectron spectrum (Ref. 10), and total fluorescence yield (Ref. 18) for CF_3Cl are included for comparative purposes. The F^- ion yield was recorded with a step size of 0.1 eV and a wavelength resolution of 6 Å. This resolution is equivalent to 0.2 eV at 20.0 eV.

Figure 3. (a) Br^- ion yield recorded following photoexcitation of CF_3Br between 12 and 28 eV. The threshold photoelectron spectrum (Ref. 10) is superimposed in red on top of the Br^- ion yield for comparative purposes. (b) I^- ion yield recorded following photoexcitation of CF_3I between 8 and 28 eV. The 8-12 eV range of this spectrum has been blown-up by a factor of 30. The threshold photoelectron spectrum (Ref. 11) is superimposed in red on top of the I^- ion yield for comparative purposes. The anion spectra are not put onto an absolute scale because the signals are shown to change non-linearly with pressure. The peak at 9.0

eV in the I^- spectrum, however, results from ion-pair formation and the cross section at this energy is 3.8×10^{-21} cm^2.

Figure 4. Cross sections for F_2^- production following photoexcitaion of CF_3Cl, CF_3Br, and CF_3I in the photon energy range 12-34 eV. The ion yields were recorded with a step size of 0.1 eV and a wavelength resolution of 6 Å. This resolution is equivalent to 0.2 eV at 20.0 eV.

Figure 5. Cross sections for FCl^- and FBr^- production following photoexcitaion of CF_3Cl and CF_3Br, respectively, in the photon energy range 12-34 eV. The ion yields were recorded with a step size of 0.1 eV and a wavelength resolution of 6 Å. This resolution is equivalent to 0.2 eV at 20.0 eV.

Figure 6. Cross sections for CF^-, CF_2^-, and CF_3^- production following photoexcitation of CF_3Cl, CF_3Br, and CF_3I in the photon energy range 10-35 eV. The ion yields were recorded with a step size of 0.1 eV and a wavelength resolution of 6 Å. This resolution is equivalent to 0.2 eV at 20.0 eV.

Figure 1.

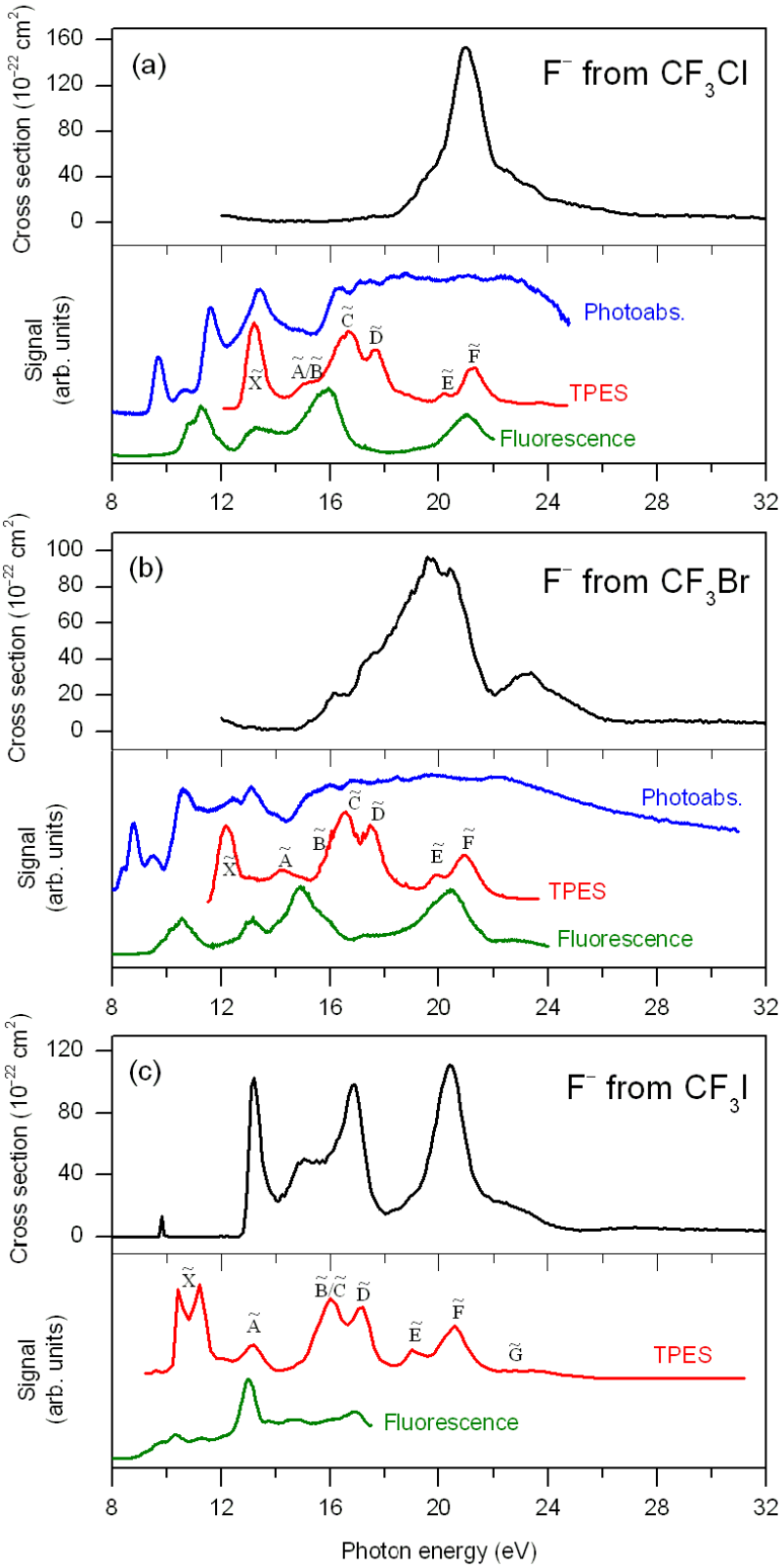
(a)
F⁻ from CF3Cl
Cross section (10⁻²² cm²)
160
120
80
40
0
Signal (arb. units)
Photoabs.
TPES
Fluorescence
X̃
Ã/B̃
C̃
D̃
Ẽ
F̃
8
12
16
20
24
28
32
(b)
F⁻ from CF3Br
Cross section (10⁻²² cm²)
100
80
60
40
20
0
Signal (arb. units)
Photoabs.
TPES
Fluorescence
X̃
Ã
B̃
C̃
D̃
Ẽ
F̃
8
12
16
20
24
28
32
(c)
F⁻ from CF3I
Cross section (10⁻²² cm²)
120
80
40
0
Signal (arb. units)
TPES
Fluorescence
X̃
Ã
B̃/C̃
D̃
Ẽ
F̃
G̃
8
12
16
20
24
28
32
Photon energy (eV)

Figure 2.

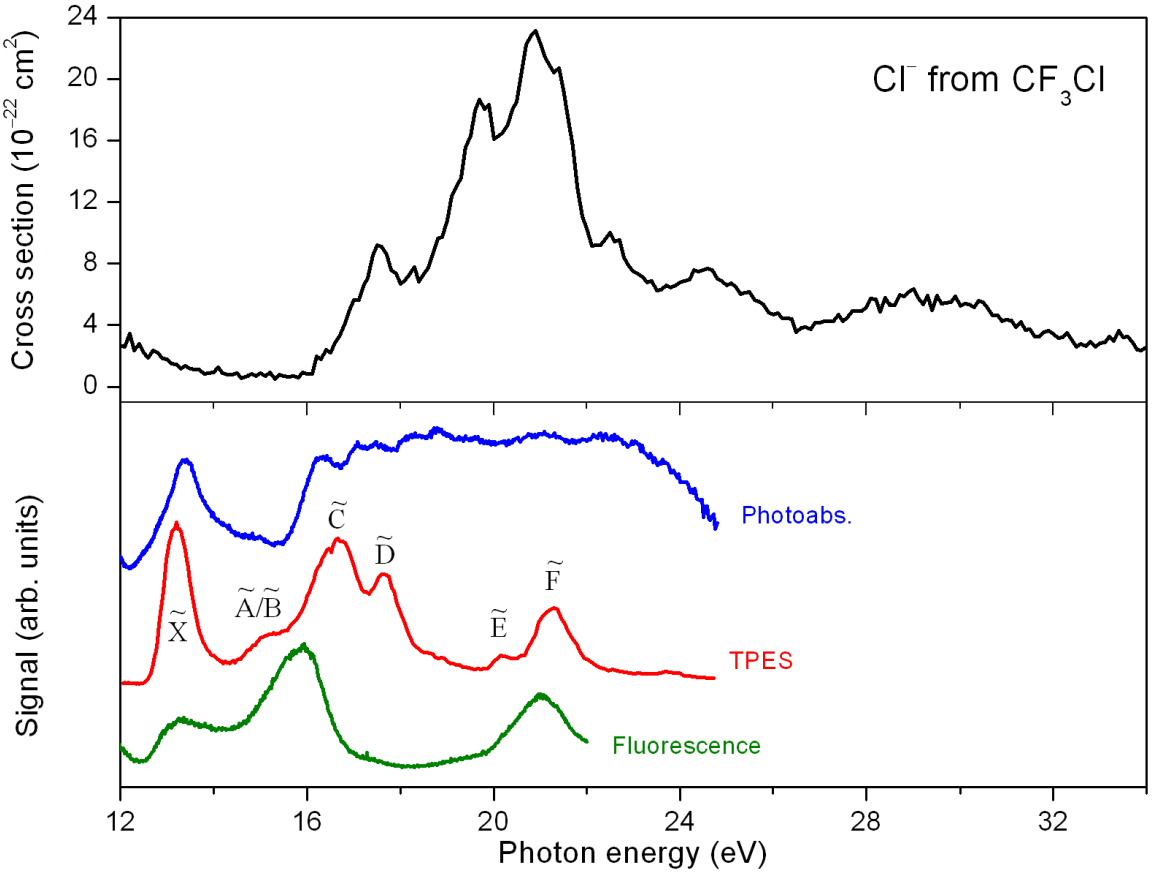
Cl⁻ from CF3Cl
Cross section (10⁻²² cm²)
Signal (arb. units)
Photoabs.
TPES
Fluorescence
X̃
Ã/B̃
C̃
D̃
Ẽ
F̃
Photon energy (eV)

Figure 3.

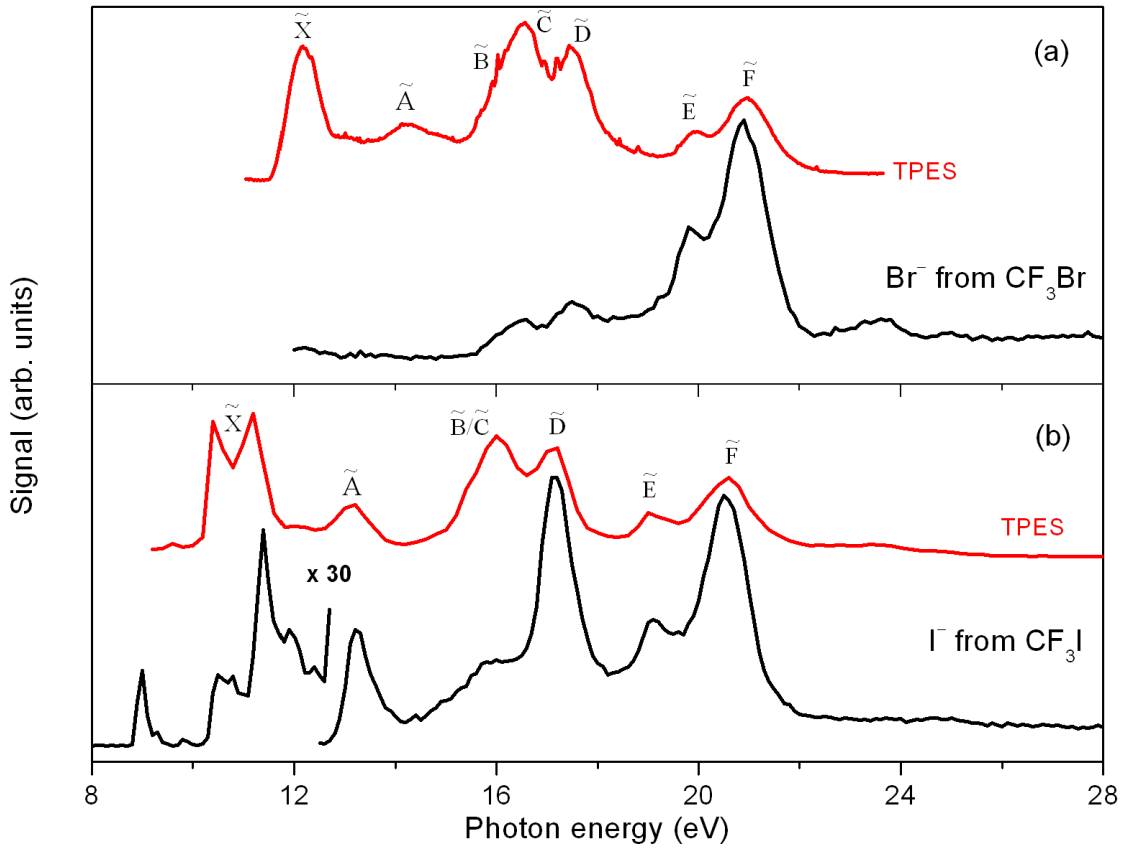
X̃
Ã
B̃
C̃
D̃
Ẽ
F̃
(a)
TPES
Br⁻ from CF3Br
X̃
Ã
B̃/C̃
D̃
Ẽ
F̃
(b)
TPES
x 30
I⁻ from CF3I
Signal (arb. units)
8
12
16
20
24
28
Photon energy (eV)

Figure 4.

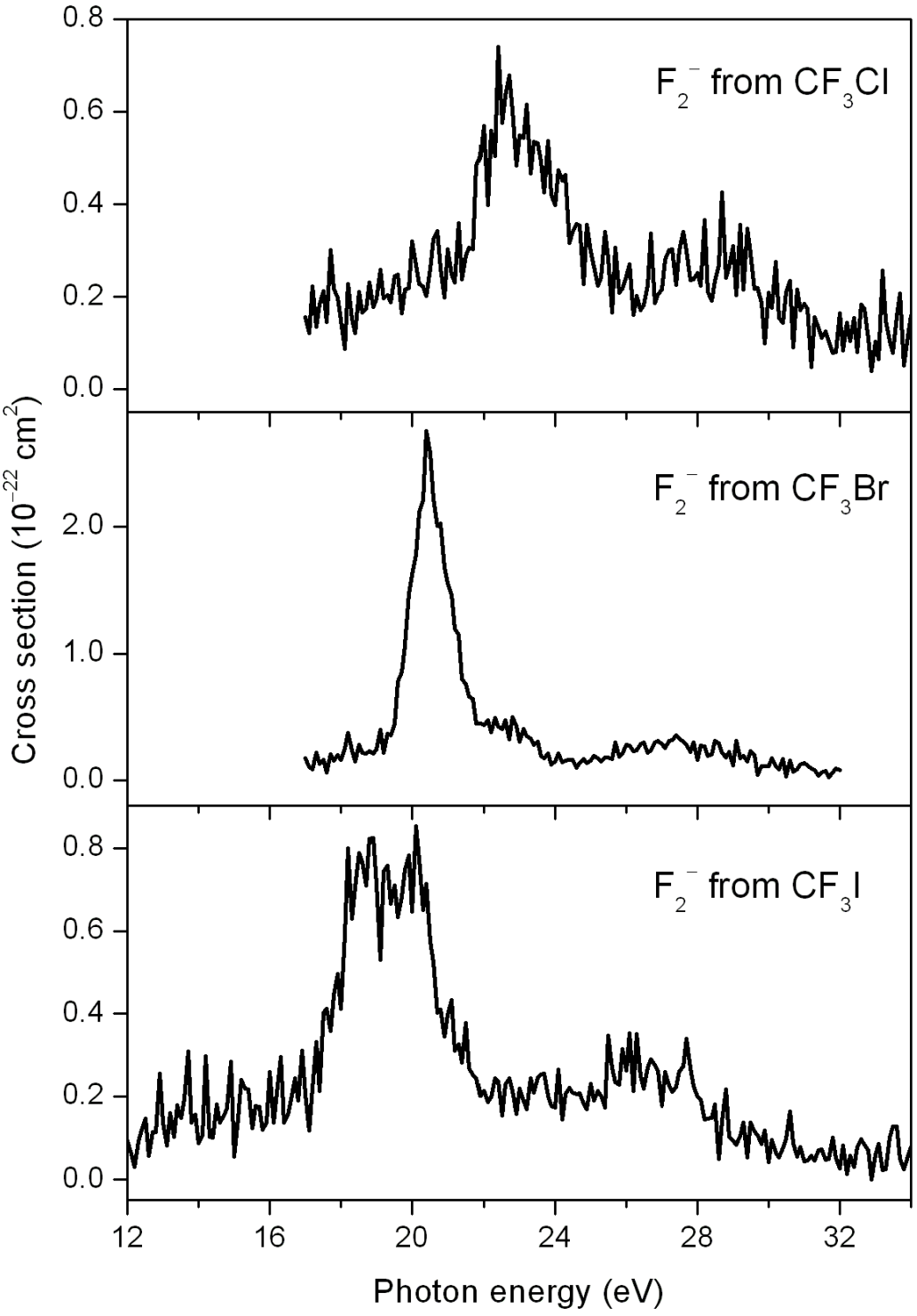
F2− from CF3Cl
F2− from CF3Br
F2− from CF3I
Cross section (10−22 cm2)
Photon energy (eV)
0.0
0.2
0.4
0.6
0.8
1.0
2.0
12
16
20
24
28
32

Figure 5.

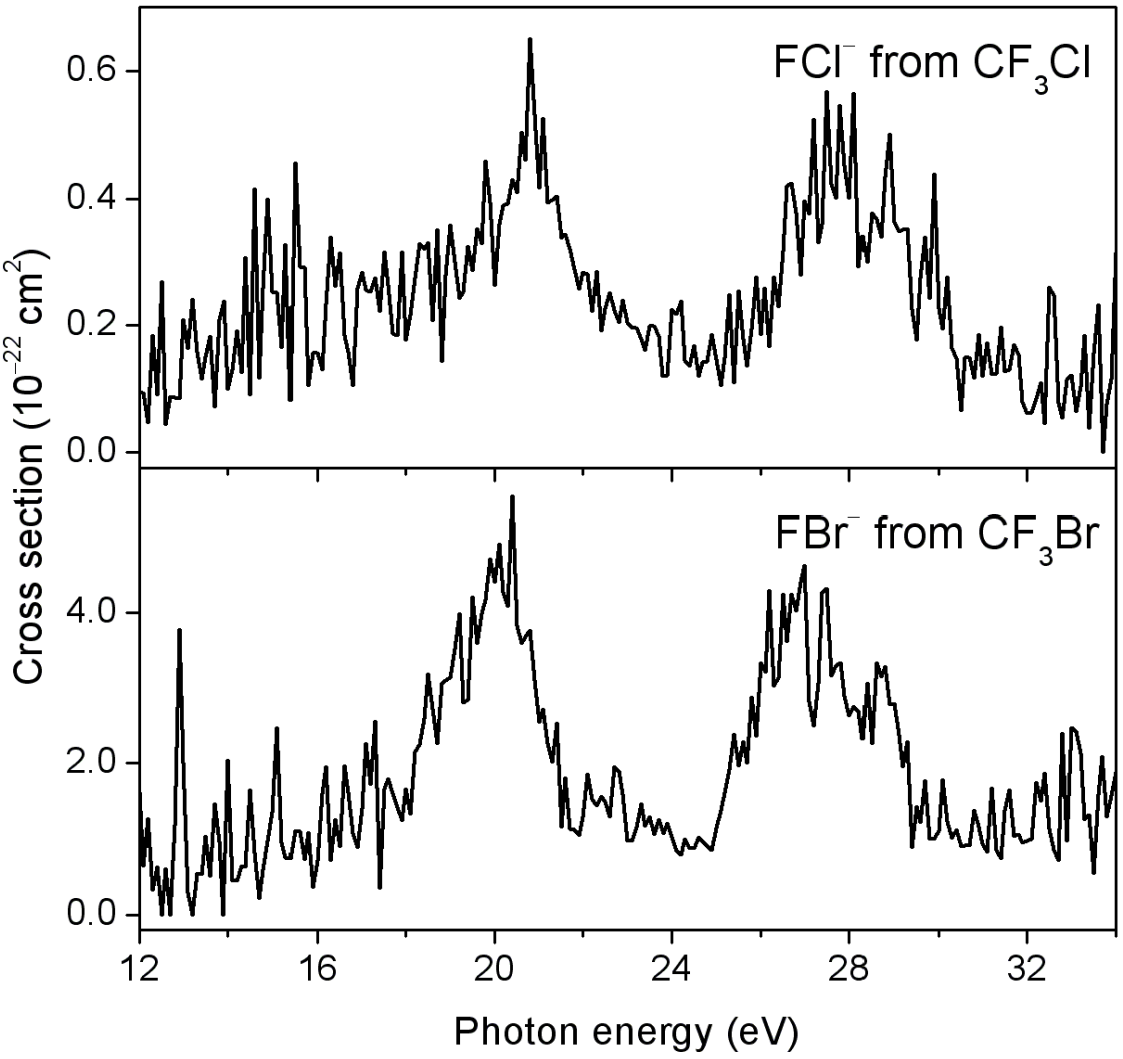
FCl⁻ from CF3Cl
FBr⁻ from CF3Br
Cross section (10⁻²² cm²)
Photon energy (eV)
0.0
0.2
0.4
0.6
2.0
4.0
12
16
20
24
28
32

Figure 6.

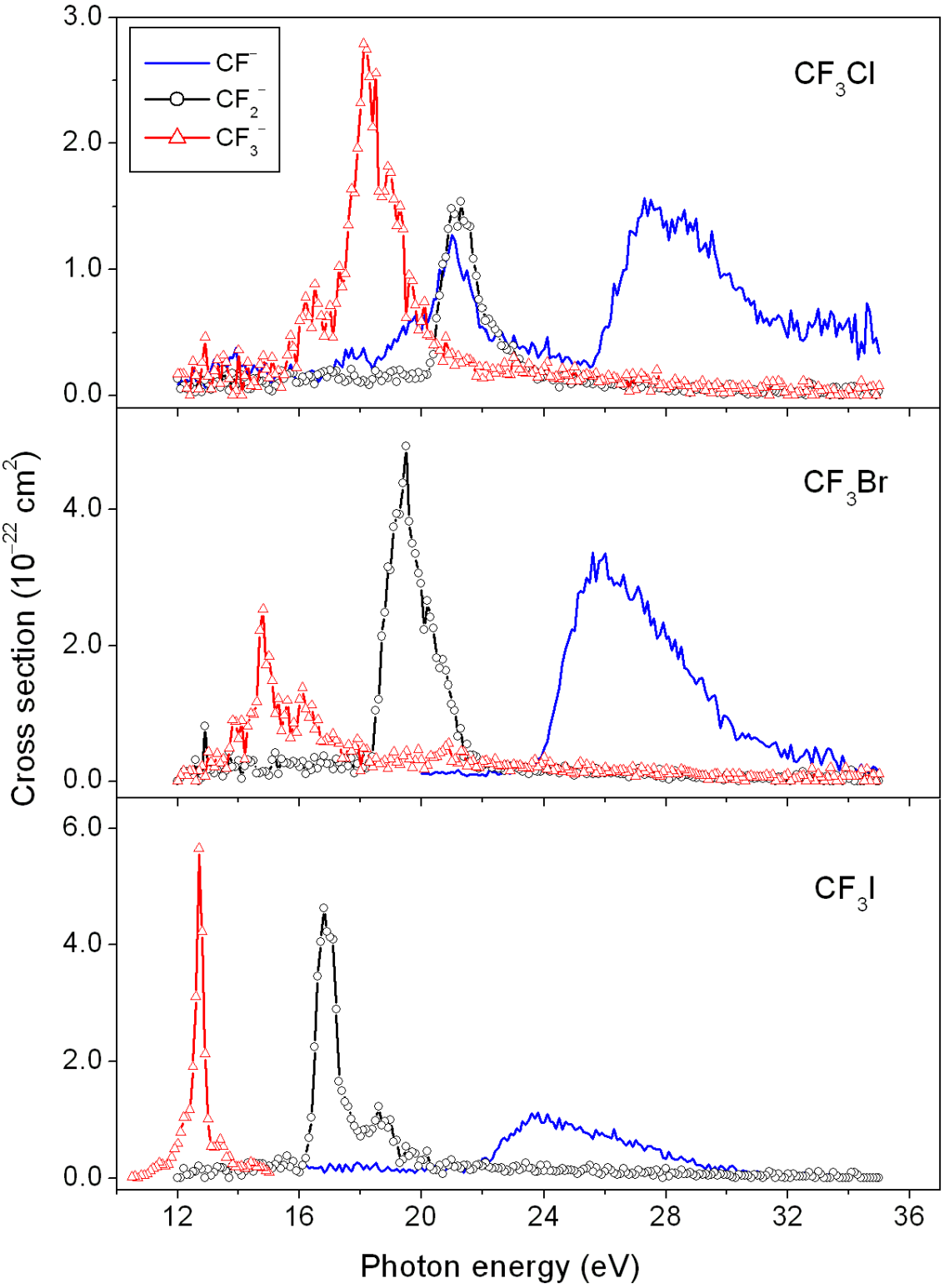
CF⁻
CF₂⁻
CF₃⁻
CF₃Cl
CF₃Br
CF₃I
Cross section (10⁻²² cm²)
Photon energy (eV)
3.0
2.0
1.0
0.0
4.0
2.0
0.0
6.0
4.0
2.0
0.0
12
16
20
24
28
32
36